Geomechanics and Engineering, *Vol. 40, No. 6 (2025) 443-457*
https://doi.org/10.12989/gae.2025.40.6.443

Evaluation of mechanical performance for sustainable glass textile reinforced cementitious composites

Liu Wei[1a], Lu Xinrong[2b], Chen Liang[2c], Deng Daping[2d], Mehdi Kouhdarag[3e] and Liang Tongxiang*[1]

[1]*Jiangxi University of Science and Technology, GanZhou 341000, Jiangxi, China*
[2]*Gannan University of Science & Technology, Ganzhou 341000, Jiangxi, China*
[3]*Department of Civil Engineering, Malekan Branch, Islamic Azad University, Malekan 5561788389, Iran*

(*Received November 11, 2024, Revised March 3, 2025, Accepted March 7, 2025*)

Abstract. This research focuses on the practical application of reinforced composites integrating glass textile within structures subjected to significant bending forces, especially in high-load-bearing flats. Every stage of preparation and testing was meticulously carried out at Jiangxi University of Science and Technology and Gannan University of Science & Technology, highlighting our dedication to advancing knowledge regarding the utilization of innovative materials in construction practices. While numerous inquiries delve into the behavior of reinforced concrete using traditional rebars, understanding the potential of composite reinforcement employing glass textile remains a critical gap. Deep comprehension of the mechanical intricacies of glass textile represents uncharted territory crucial for pioneering structural advancements. This article aims to establish an innovative framework for exploring glass textile as a viable composite reinforcement. The meticulous orchestration of tests, including the mini-slump test, sets a pioneering precedent for nuanced experimentation. Also, assessments via the compressive strength test and the three-point bending test significantly contribute to our understanding of the material's behavior, fostering a paradigm shift in utilizing reinforced composites in high-stress structural settings.

Keywords: deflection hardening; deflection softening; flexural strength; GGBFS; Glass textile

1. Introduction

Composite materials combine different materials to address individual weaknesses, such as stiffness and durability in concrete. Researchers explore innovative methods using external materials to enhance these properties. Fibers, especially, play a crucial role in reinforcing composites (Lho *et al*. 2012, Khan *et al*. 2024). A variety of fibers are used in concrete, categorized as continuous or discontinuous. Continuous fibers, with higher stiffness and strength albeit at a higher cost, are preferred due to their long aspect ratio, aka, length-to-diameter ratio (Wang *et al*. 2019, Kansal and Goyal 2021). Materials like basalt, glass, and carbon fibers are common in structural applications for their high strength and modulus (Amin *et al*. 2022, Wu *et al*. 2024). Continuous textile fibers, in particular, are favored for their durability, strength, and cost-effectiveness, making them essential in optimizing concrete performance (Türkmen *et al*. 2003, Benimam *et al*. 2021, Penelope *et al*. 2023).

Composite materials are categorized into polymeric matrix composites (PMCs), ceramic matrix composites (CMCs), and Mortar Matrix Composites (MMCs), with CMCs and MMCs particularly important in structural applications. Research focuses on improving their weaknesses like low tensile strength, fracture toughness, and susceptibility to cracking. Initially, steel fibers were used to prevent crack propagation but affected concrete workability (Luo *et al*. 2019, Liao *et al*. 2021). Recent advancements favor continuous elements like ferrocement, showing significant improvements in tensile strength and post-peak response (Marthong 2019, Wu *et al*. 2022). This innovative approach marks a transformative step in enhancing concrete and mortar performance, promising to overcome traditional reinforcement limitations (Pan *et al*. 2024, Hang *et al*. 2024, Liu *et al*. 2024).

Ground granulated blastfurnace slag (GGBFS) is a byproduct from iron production, combining iron and slag containing lime, silica, and alumina (Guleria and Salhotra 2016). Research highlights its ability to enhance concrete's durability, strength, and workability, often replacing Portland cement in certain ratios (Khanzadi and Behnood 2009, Liu *et al*. 2020). GGBFS is formed by rapidly cooling molten blastfurnace slag, then ground to increase reactivity, enhancing cement hydration and C-S-H gel formation (Nanehkaran *et al*. 2023). Its inclusion in concrete improves structural integrity, reduces creep and drying shrinkage post-casting (Geo *et al*. 2018, Liu *et al*. 2020). Richardson (2006) notes GGBFS initially lowers early strength but improves long-term strength and offers other benefits like reducing chloride permeability, diminishing creep, enhancing sulfate and alkali-silica resistance, improving

*Corresponding author, Professor
E-mail: liangtx0729@163.com
[a]Associate Professor
[b]Professor
[c]Associate Professor
[d]Professor
[e]Assistant Professor

ISSN: 2005-307X (Print), 2092-6219 (Online)

workability, reducing bleeding, lowering hydration heat, and increasing steel corrosion resistance.

Research underscores the benefits of integrating Ground Granulated Blast Furnace Slag (GGBFS) into concrete, enhancing durability, strength, and overall performance of structures. Investigating glass textile reinforced cementitious composites represents pioneering work in construction materials, combining high tensile strength and durability with cement-based matrices to surpass traditional reinforcements (Mindess and Bentur 1990). This approach improves strength, crack resistance, and potentially extends structure lifespan, evaluated through advanced testing methods (Olivito and Zuccarello 2010). These composites strengthen cement with glass fibers, enhancing durability and corrosion resistance, though challenges include cement brittleness and fiber-matrix adhesion (Noghabai 2000, Noshiravani and Brühwiler 2013). Understanding both strengths and limitations is critical for efficient use in construction (Altun *et al*. 2006). Glass textile fibers, lightweight with exceptional strength and durability, offer robust reinforcement and affordability for various applications, with weaving methods enhancing their versatility (Mobasher 2011).

2. Materials and methods

This research aims to extensively investigate and enhance the quality of Glass Textile Reinforced Cementitious Composites (GTRCC) through detailed laboratory experiments. It is focused on refining properties and optimizing performance and durability using innovative methods. The study meticulously examines material composition, manufacturing processes, and structural performance to improve mechanical properties and overall quality. Through systematic experimentation, the goal is to contribute novel insights and advancements in GTRCC, making them more suitable for diverse engineering and construction applications.

2.1 Sample preparation

The preparation of composite mixtures in cement-based materials involves a systematic and careful process, crucial for ensuring the final concrete meets stringent quality and performance requirements. This meticulous procedure begins with the selection of materials. Cement, aggregates, and reinforcements such as fibers or additives are chosen based on the desired properties of the concrete. The accurate measurement and batching of these materials in precise proportions are fundamental, ensuring consistency and uniformity in the final composite. The mixing process is a critical phase where dry components like cement and aggregates are blended in predetermined ratios. Water is gradually added to activate the cement and achieve the required workability. This meticulous mixing process can be executed using different methods, including manual hand mixing, machine mixing in conventional drum mixers, or specialized equipment for larger-scale projects. Reinforcements like fibers or additives such as Ground Granulated Blast-Furnace Slag (GGBFS) are introduced during mixing, adhering to predetermined proportions to impart specific properties to the composite mixture. Quality control is paramount throughout the preparation process. Regular testing of the composite mixture ensures its workability, setting time, strength, durability, and adherence to specific performance criteria. Adjustments to the mix design might be made based on test results to fine-tune the material's properties. Adherence to industry standards and specifications remains essential to ensure the composite mixture aligns with required quality benchmarks, guaranteeing the reliability and performance of the final concrete product.

2.2 GTRCC mix design

Throughout this experimental investigation, we meticulously explored two distinct ratios of GGBFS within the composite mixture: 30% and 40% of the total cement volume. Determination of these proportions relied on the minislump test, a crucial assessment aimed at identifying the most optimal flow rate for the composite. The detailed properties of the composite mixture are thoroughly outlined in Table 1 for comprehensive reference. It's important to note that exclusively quartz aggregate with a maximum particle size (D_{max}) of 400μm was employed in this research. Additionally, to provide a comprehensive understanding, the physical and chemical attributes of the cement used in this study are meticulously detailed in Tables 2 and 3 respectively, offering a comprehensive overview of its properties and characteristics for reference and comparison purposes.

2.3 Compressive strength test

The compressive strength test is crucial for evaluating concrete's load-bearing capacity and durability. It involves subjecting cylindrical or cubical specimens to increasing compressive forces until they fracture. Specimens are carefully collected and cured to optimize strength development through hydration (Mudadu *et al*. 2019). This test provides essential data on concrete quality and adherence to construction standards, ensuring structures can safely bear anticipated loads (Doyon-Barbant and Charron 2018). The uniaxial compressive strength test, UCS (Cemiloglu *et al*. 2023), following ASTM C39/C39M standard, uses cylindrical specimens prepared from concrete batches. After controlled curing, specimens are tested by applying increasing compressive force until failure, recording load, deformation, and failure mode (Travush *et al*. 2020). Strict adherence to ASTM guidelines is essential for accurate and reliable results (Hassan *et al*. 2012). Two improved mix designs were tested with mortar samples, cured and tested after seven days to assess compressive strength (Bencardino *et al*. 2010). Results are summarized in Table 4 for further analysis and comparison.

2.3 Flexural strength test

The flexural strength test, also known as the bending

Table 1 Properties of concrete mixtures that used in this study

No.	Sample ID	C (kg/m^3)	W (kg/m^3)	GGBFS (kg/m^3)	S (kg/m^3)	SP (kg/m^3)	TV (kg/m^3)	W/B	SP/B	S/B
1	0.1G	812.4	366.8	206.6	817.4	8.0	2152.3	0.39	0.80	0.80
2	0.2G	798.2	359.4	215.8	805.8	7.9	2165.9	0.37	0.79	0.79
3	0.3G	792.8	356.8	237.8	792.8	7.9	2188.1	0.35	0.77	0.77
4	0.4G	771.8	347.3	308.7	771.8	7.7	2207.3	0.32	0.71	0.71
5	0.5G	765.8	342.2	312.9	765.3	7.7	2212.8	0.30	0.70	0.70
6	0.6G	761.3	336.3	329.7	760.3	7.7	2234.1	0.27	0.69	0.69
7	0.7G	760.8	319.7	336.7	692.8	7.1	2245.4	0.25	0.67	0.67
8	0.8G	758.7	310.0	351.2	671.8	7.1	2259.6	0.22	0.65	0.65
9	0.9G	745.7	308.8	359.8	665.9	7.0	2267.3	0.20	0.65	0.65
10	0.10G	742.8	302.6	360.4	660.3	7.0	22778.1	0.20	0.61	0.61

Note: C is Cement, W is Water, S is Sand, SP is Superplasticizer, TV is Total Volume

Table 2 Physical properties of Portland cement that used in this study

Characteristic	Unit	Value
Density	kg/m^3	3110
Blaine fineness	cm^2/g	3280
Time of setting (Vicat test), initial set	min	203
Time of setting (Vicat test), final set	min	285
Volume stability (Le-Chatelier)	mm	3

Table 3 Chemical properties of Portland cement that used in this study

Characteristic	Unit	Value
SiO_2	%	20.84
Al_2O_3	%	4.27
Fe_2O_3	%	3.66
CaO	%	63.92
MgO	%	1.12
SO_3	%	2.63
Insoluble residue	%	0.67
Loss on ignition	%	1.90
Free lime	%	0.89

test or modulus of rupture test, assesses how materials respond to bending stresses, crucial for beams, slabs, and other structural elements (Yoo *et al*. 2019). Standard procedures, like ASTM C78 for concrete, dictate preparation of rectangular prismatic specimens, subjected to increasing loads at the center of a span between supports. Measurements of load and deformation during the test inform calculations of flexural strength, indicating a material's ability to resist bending forces (Tailhan *et al*. 2012, Xu *et al*. 2020). This test method, essential in construction and engineering, ensures structural integrity and guides resilient design and construction practices (Arunakanthi and Kumar 2016). To assess the bending strength of composite materials, wooden molds measuring 20mm×300mm×300mm were meticulously prepared. These molds were outfitted with two distinct layers of glass, introducing variability in the composition of the composites. The specific properties of the glass textile utilized in this experiment are comprehensively outlined in Table 5 for reference and analysis. Following the demolding process, the samples underwent a curing phase lasting 28 days under controlled laboratory conditions, allowing for the concrete to mature and develop optimal strength properties. Subsequently, the flexural strength test, also known as the modulus of rupture test, was conducted on the samples according to the ASTM A-360 standard specifications. The test was carried out with a controlled speed rate set between 1.00 to 1.50 mm/min.

This standardized test method evaluates a material's resistance to bending stresses, crucial for understanding its structural integrity and load-bearing capacity. Detailed specifications regarding the flexural test samples and the

Table 4 The compressive strength test result provided in this study without any additives

No.	Sample ID	Maximum Load (KN)			Compressive strength (MPa)		
		Stage 1	Stage 2	Stage 3	Stage 1	Stage 2	Stage 3
1	0.1G	38.4	38.9	38.9	24.22	25.76	25.76
2	0.2G	40.2	41.8	41.8	25.03	26.04	26.04
3	0.3G	40.2	41.8	41.8	25.12	26.12	26.12
4	0.4G	51.8	51.5	51.5	33.37	32.87	35.30
5	0.5G	52.4	53.7	53.7	34.53	34.75	34.75
6	0.6G	55.6	56.2	56.2	36.91	37.12	37.12
7	0.7G	58.4	59.4	59.4	37.45	39.55	39.55
8	0.8G	63.1	63.9	63.9	39.88	41.29	41.29
9	0.9G	63.1	63.9	63.9	39.85	41.29	41.29
10	0.10G	65.4	66.4	66.4	40.56	43.63	43.63

Table 5 Properties of utilized glass textile in this experiment (Note: Information adapted from supplier)

Description	Unit	AR 380		Tolerance	Analysis method	AR 380		Tolerance	Analysis method
Final weight	g/m^2	215		0.05	DIN EN 12127	340		0.05	DIN EN 12127
Coating	g/m^2	38		0.05	DIN EN 12127	57		0.05	DIN EN 12127
		Warp	Weft			Warp	Weft		
Aperture size	mm	45	44	0.2	DIN EN 12127	34.5	27.6	0.2	DIN EN 12127
Yarn count	Yarns/10 cm	2.0	2.0	0.5		2.5	3.0	0.5	
Tensile strength	N/5 cm	1800	2300	-	DIN EN ISO 13934-1	2900	2900	-	DIN EN ISO 13934-1
Elongation	%	3.5	3.9			3.0	2.95		
Coating type	PVAC					PVAC			

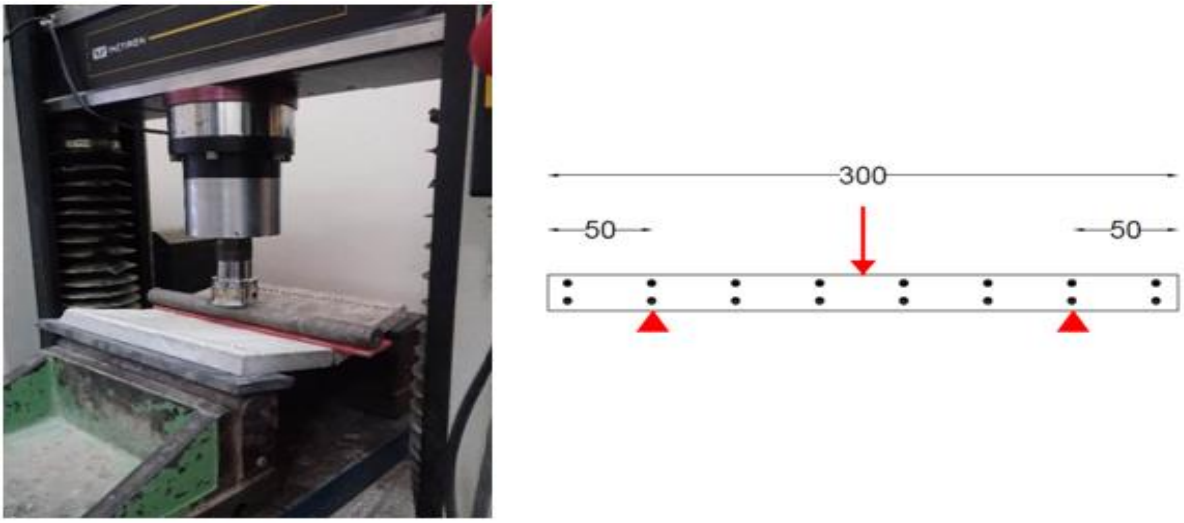

Fig. 1 A detail scheme and view of flexural strength test that used in this study

testing setup are elaborated in Fig. 1, offering a comprehensive visual representation of the experimental configuration and test procedures utilized in the assessment of the composite materials' bending strength. It should be noted that all stages of preparation and testing were meticulously undertaken at Jiangxi University of Science and Technology and Gannan University of Science & Technology, underscoring our commitment to advancing the knowledge base regarding the application of cutting-edge materials in construction practices.

This test was designed to explore the behavior and efficacy of textile materials in two distinct orientations:

Table 6 The compressive strength test result for GGBFS mixed composite

No.	Sample ID	Maximum Load (KN)			Compressive strength (MPa)		
		Stage 1	Stage 2	Stage 3	Stage 1	Stage 2	Stage 3
1	0.1G-2	40.6	41.6	41.6	26.16	27.56	27.56
2	0.2G-2	45.2	47.2	47.2	27.52	29.03	29.03
3	0.3G-2	45.5	47.5	47.5	29.11	31.25	31.25
4	0.4G-2	53.7	55.6	55.6	35.45	36.97	36.97
5	0.5G-2	59.6	60.9	60.9	36.52	38.06	38.06
6	0.6G-2	61.7	62.8	62.8	37.73	39.34	39.34
7	0.7G-2	63.5	65.1	65.1	39.87	41.40	41.40
8	0.8G-2	65.6	66.6	66.6	41.25	45.71	45.71
9	0.9G-2	65.6	66.6	66.6	41.25	45.71	45.71
10	0.10G-2	69.4	70.5	70.5	43.60	46.98	46.98

longitudinal (referred to as "L") and transverse (indicated as "T"). Within this thesis, the longitudinal direction is identified as "L", while the transverse direction is denoted by "T." For instance, a composite labeled as 0.3G/680/T signifies a specific mix design of 0.3G, utilizing glass textile code AR680, with the test orientation set in the transverse direction. This nomenclature system serves as a clear and systematic method for specifying the composite compositions and orientations tested in this research study.

The flexural strength test, also known as the modulus of rupture or bending test, is essential for evaluating composite concrete reinforced with GGBFS. This test helps understand how the composite material behaves under bending stresses, providing crucial insights into its structural integrity and performance. In this test, rectangular beam or bar specimens of composite concrete with GGBFS are subjected to control loading at the midpoint until they fail due to bending stress. Assessing the flexural strength of this material is vital to ensure it meets required standards for structural applications such as beams and slabs, confirming its ability to resist bending forces without failure. Evaluating flexural strength also helps determine the material's reliability and quality, aiding in material selection and optimizing design considerations for this specific composite. The test data predicts the material's behavior under bending loads and identifies potential failure modes like tension, compression, or shear. This information is crucial for engineers to design structures that can withstand various stresses, ensuring safety and durability. Additionally, the flexural strength test supports the development of composite concrete formulations with GGBFS, enabling researchers to improve the material's bending properties and maintain consistent quality across different industries.

3. Results

Table 6 presents the results of the compressive strength test, giving a detailed overview of the material's ability to withstand compression and its overall load-bearing capacity. The flexural strength test results are shown in Figs. 2 to 6, providing graphical representations of the material's performance under bending stresses. These figures illustrate the varying outcomes of the flexural strength tests, allowing for a visual comparison of the material's behavior under different conditions. Together, the data from Table 6 and the graphical insights from Figs. 2 to 6 offer a comprehensive understanding of the material's structural integrity, aiding in structural design and material selection.

Table 7 provides a detailed summary of ultimate energy absorption data from the average load-deflection curvature observed during the flexural strength test. It also includes the percentage of total textile volume relative to the composite's volume, offering a comprehensive view of the energy absorption capabilities and textile volume ratios across the different composite mixtures. The load-deflection behavior after the first crack, known as the "BOP," shows two distinct classifications: "deflection-softening" and "deflection-hardening." Another important parameter is the maximum load point after the first crack or BOP, called the "Modulus of Rupture (MOR)." Table 8 provides a summary of the BOP and MOR values along with the response behaviors observed in each composite.

Figs. 7 and 8 compare the flexural strength of the original matrix with that of the composite reinforced with glass textile. These figures illustrate how textile reinforcement enhances the material's structural behavior. This analysis is crucial for engineering applications, guiding optimized material selection and improved structural design, especially for cement-based composites. Key observations include:

- For the weaker matrix (0.3G), the maximum load capacity increases from about 2.743 N/mm² to 6.739 N/mm² with textile reinforcement (0.3G/680) and even higher to 7.725 N/mm² (0.3G/370).
- For the stronger matrix (0.4G), the maximum load capacity is 8.95 N/mm², with minimal change when reinforced.

These findings highlight that textile reinforcement significantly boosts flexural strength in weaker matrices (180% increases for 0.3G) but shows negligible

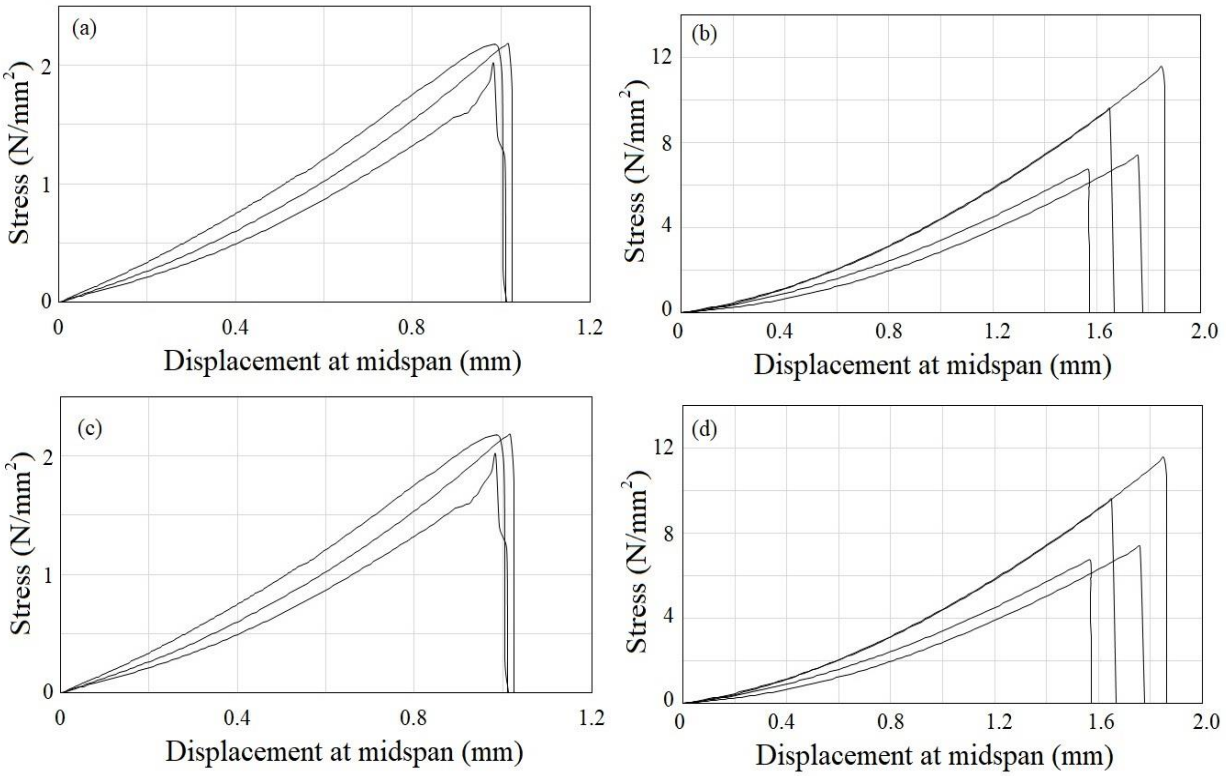

Fig. 2 Flexural strength test results of several samples: (a) 0.3G, (b) 0.4G, (c) 0.2G and (d) 0.5G

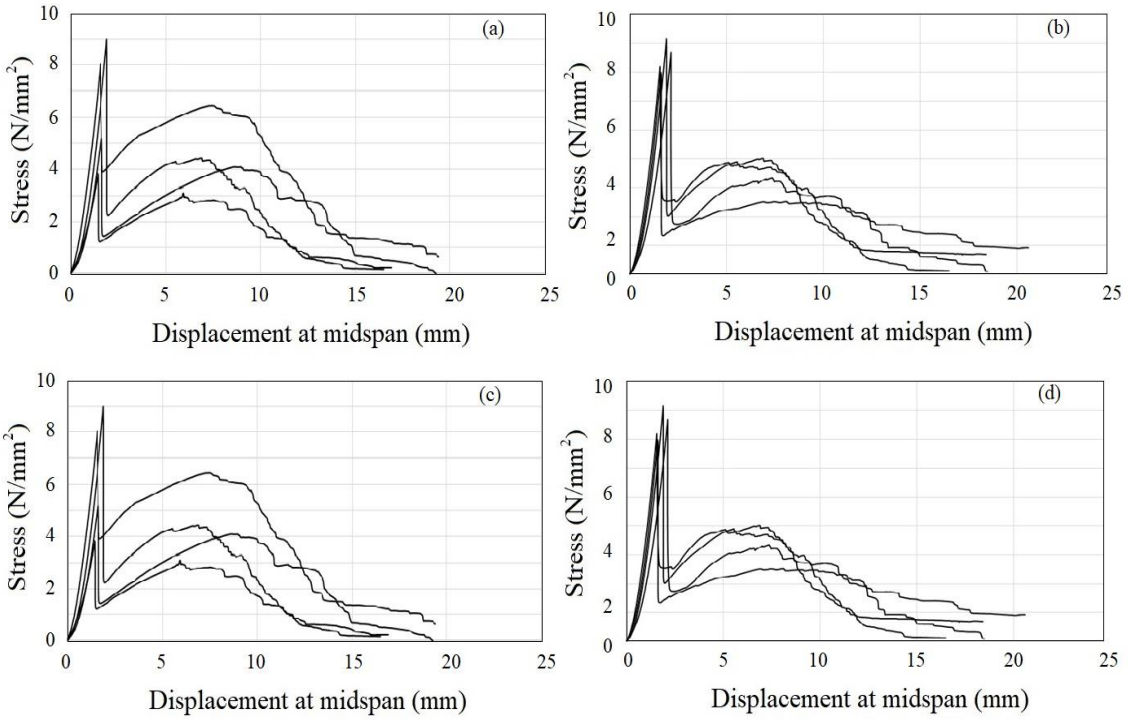

Fig. 3 Flexural strength test results of selected samples (a) 0.1G/680/T, (b) 0.2G/680/L, (c) 0.3G/680/L and (d) 0.4G/680/L

improvement in stronger matrices (0.4G). Additionally, composites with weaker matrices exhibit higher mid-span deflection values, indicating better bond behavior between the matrix and textile, allowing for increased deformation. The study uses two types of glass textiles, AR 680 and AR 370, as detailed in Table 5. Figs. 8 and 9 show the specific effects of these textile types on flexural strength. Figs. 10 to 15 offer comprehensive insights into how varying matrix

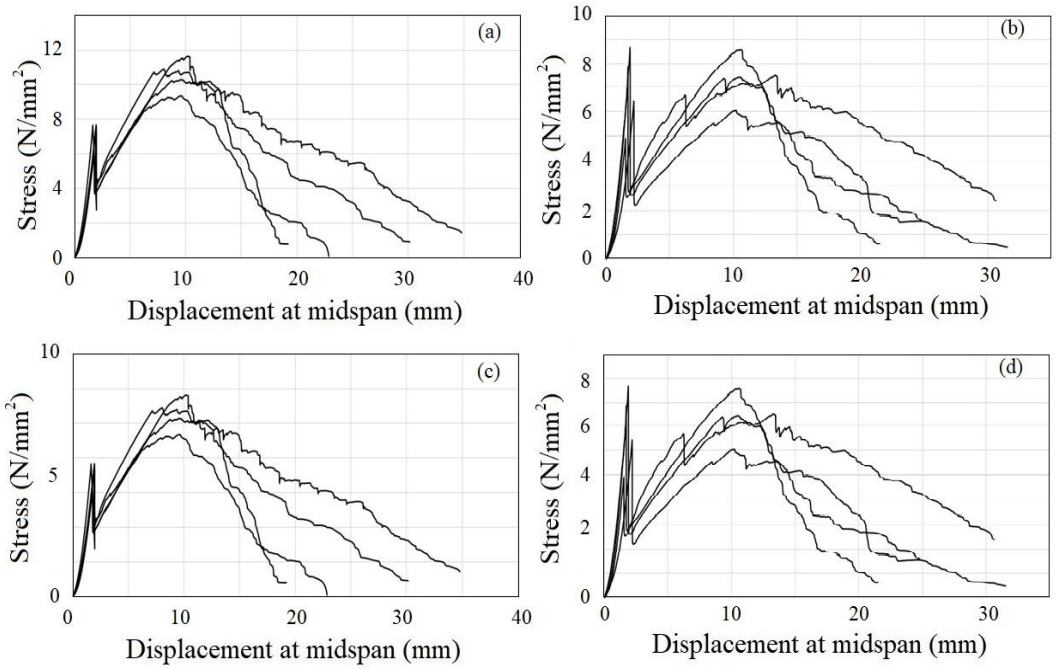

Fig. 4 Flexural strength test results of selected samples (a) 0.1G/370/T, (b) 0.4G/370/T, (c) 0.4G/370/T and (d) 0.4G/370/L

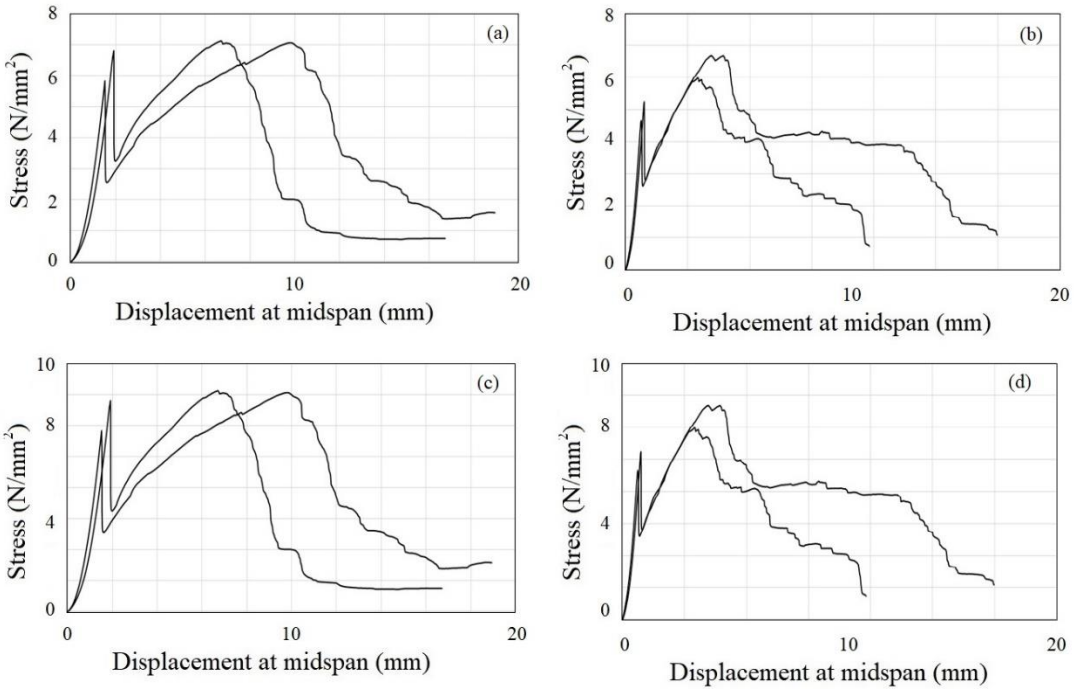

Fig. 5 Flexural strength test results of selected samples (a) 0.1G/310/T, (b) 0.2G/310/L, (c) 0.3G/310/L and (d) 0.4G/310/L

mix proportions affect the flexural strength of composites, highlighting distinct behaviors and responses. In weaker matrix composites, AR 680 reinforcement showed higher fracture energy compared to AR 370, particularly evident in the 0.3 mix proportion where AR 680 exhibited pullout behavior leading to increased mid-span deformation. Figure 12a indicates enhanced bonding characteristics in these scenarios, improving load capacity during strain-hardening phases. The comparison between AR 680 and AR 370 in. weaker matrix composites underscores AR 680's superior performance in fracture energy and mid-span deformation dynamics.

4. Discussion

The bond strength between the matrix and textiles, termed 'bond strength,' determines whether textiles

Table 7 Summarized of energy absorption and textile volume

Sample ID	Ultimate energy absorption (N/mm)	Standard deviation of energy absorption (N/mm)	V_f (mm^3)
0.1G	0.95	0.26	-
0.2G	1.00	0.37	-
0.3G	1.05	0.25	-
0.4G	4.8	0.25	-
0.5G	4.8	0.77	-
0.6G	5.3	0.76	-
0.7G	5.6	0.63	-
0.8G	5.9	0.75	-
0.9G	6.7	0.81	-
0.10G	6.7	0.81	-
0.1G/680/L	87.67	0.075	0.55%
0.1G/680/T	75.93	1.17	0.55%
0.1G/370/L	107.16	0.97	1.38%
0.1G/370/T	167.85	12.12	1.38%
0.2G/680/L	85.43	25.96	0.55%
0.2G/680/T	60.17	0.41	0.55%
0.2G/370/L	155.44	4.89	1.38%
0.2G/370/T	169.25	17.15	1.38%
0.3G/680/L	91.80	32.05	0.55%
0.3G/680/T	63.78	15.65	0.55%
0.3G/370/L	147.68	30.66	1.38%
0.3G/370/T	167.88	0.077	1.38%
0.4G/680/L	37.92	4.72	0.55%
0.4G/680/T	45.77	18.92	0.55%
0.4G/370/L	106.39	14.50	1.38%
0.4G/370/T	157.45	36.78	1.38%
0.5G/680/L	25.74	45.36	0.55%
0.5G/680/T	49.26	23.58	0.55%
0.5G/370/L	149.23	1.78	1.38%
0.5G/370/T	170.20	0.81	1.38%

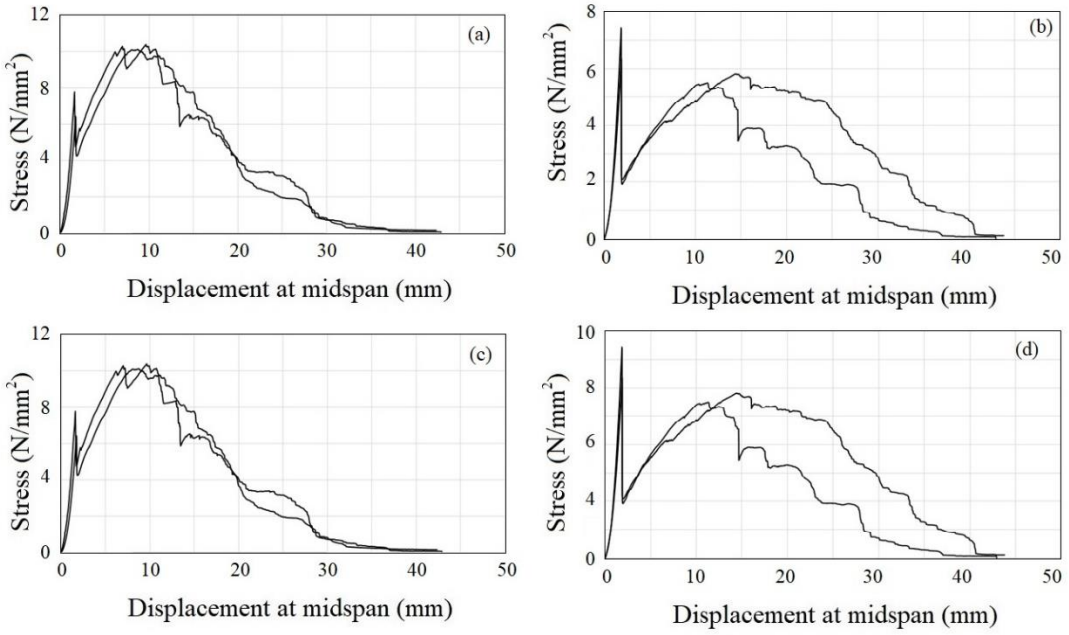

Fig. 6 Flexural strength test results of selected samples (a) 0.1G/250/T, (b) 0.4G/250/T, (c) 0.4G/250/T and (d) 0.4G/250/L

Table 8 BOP and MOR values and response behavior of composite obtained from flexural strength tests

Sample ID	BOP (N/mm^2)	MOR (N/mm^2)	Response behavior
0.1G	1.798, 1.658, 1.572	-	-
0.2G	2.932. 2.854, 2.763	-	-
0.3G	2.178, 2.743, 2.006	-	-
0.4G	6.130, 7.073, 6.434	-	-
0.5G	8.129, 6.951, 4.012	-	-
0.6G	7.654, 6.598, 4.259	-	-
0.7G	6.389, 6.542, 5.451	-	-
0.8G	6.220, 5.879, 6.110	-	-
0.9G	7.852, 8.107, 7.859	-	-
0.10G	7.653, 7.455, 7.707	-	-
0.1G/680/L	3.586, 3.489, 3.486	3.410, 2.596, 2.045	Deflection-softening
0.1G/680/T	4.568, 5.716, 5.469	4.257, 4.005, 4.694	Deflection-softening
0.1G/370/L	4.976, 4.569, 5.865	4.232, 4.010, 5.207	Deflection-softening
0.1G/370/T	9.124, 7.489, 5.456	7.561, 6.888, 5.400	Deflection-softening
0.2G/680/L	3.696, 4.587, 4.206	4.596, 3.497, 3.521	Deflection-hardening, Deflection-softening,
0.2G/680/T	5.621, 5.367, 5.149	6.654, 6.961, 6.753	Deflection-hardening
0.2G/370/L	7.456, 7.583, 7.195	8.794, 8.508, 8.665	Deflection-hardening
0.2G/370/T	6.394, 6.453, 6.555	5.521, 5.260, 4.106	Deflection-softening
0.3G/680/L	4.578, 5.195, 5.780	6.666, 5.898, 5.840	Deflection-hardening
0.3G/680/T	6.739, 5.711, 5.149	7.098, 7.059, 7.120	Deflection-hardening
0.3G/370/L	7.146, 7.635, 6.195	5.608, 5.964, 4.575	Deflection-softening
0.3G/370/T	6.360, 6.597, 5.146	6.875, 7.159, 4.238	Deflection-hardening, Deflection-softening
0.4G/680/L	7.651, 7.685, 7.158	4.011, 2.501, 3.845	Deflection-softening
0.4G/680/T	8.952, 5.185, 5.012	4.422, 4.075, 3.250	Deflection-softening
0.4G/370/L	4.835, 8.452, 6.126	7.536, 5.594, 5.756	Deflection-hardening, Deflection-softening
0.4G/370/T	7.584, 7.616, 6.458	10.481, 11.267, 10.275	Deflection-hardening
0.5G/680/L	7.815, 6.391, 7.265	5.521, 3.285, 3.299	Deflection-softening
0.5G/680/T	6.548, 6.147, 7.259	8.219, 9.128, 9.637	Deflection-hardening
0.5G/370/L	3.459, 4.876, 4.521	3.127, 6.129, 6.127	Deflection-softening, Deflection-hardening
0.5G/370/T	9.145, 9.147, 9.753	10.258, 11.208, 10.896	Deflection-hardening

experience rupture or pullout, influencing overall composite performance. This segment aims to explore how matrix mix proportions impact flexural strength through microscopic examination of damaged textiles and comparison of flexural strength test results across different matrix compositions. The results' figures provide a detailed analysis of how different types of textiles affect the flexural strength of composite materials. They reveal valuable insights into how AR 370 and AR 680 textiles impact the overall performance of the composite. Specifically, AR 370 demonstrates higher load-bearing capacity and greater deflection compared to AR 680. The energy absorption, as indicated by the stress-deflection curve area, is directly influenced by the textile type and its composition, with AR 370 outperforming AR 680 in this study. The bonding quality between the textile and matrix plays a crucial role, notably stronger in AR 370 than in AR 680, which contributes significantly to the observed outcomes. Moreover, the quantity of fibers within the textile becomes pivotal, especially in robust matrices like 0.4G.

In cement-based composites, the ultimate strain capacity of textiles surpasses that of the matrix, leading to the matrix failing earlier than the composite as a whole once the textile reaches peak tensile stress. The textile acts as a bridge over cracks and continues to bear additional loads after cracking, with the matrix gradually transferring load to the textiles. Introducing glass textile into 0.3G composite mixes significantly increased the matrix failure load compared to the plain matrix. Specifically, incorporating glass textile in the 0.3G matrix nearly doubled the Bend Over Point (BOP) value across the mixtures. This clearly demonstrates that adding glass textile enhances the matrix's strength, particularly in achieving higher failure strength. Upon reaching matrix failure, all composites showed a sudden performance decline, similar to the 0.4G mixture. However, distinct response patterns emerged among the 0.3G composites. The 0.3G/370/L composite displayed a deflection-softening pattern, while the 0.3G/680/L, 0.3G/680/T, and 0.3G/370/T composites exhibited deflection-hardening characteristics.

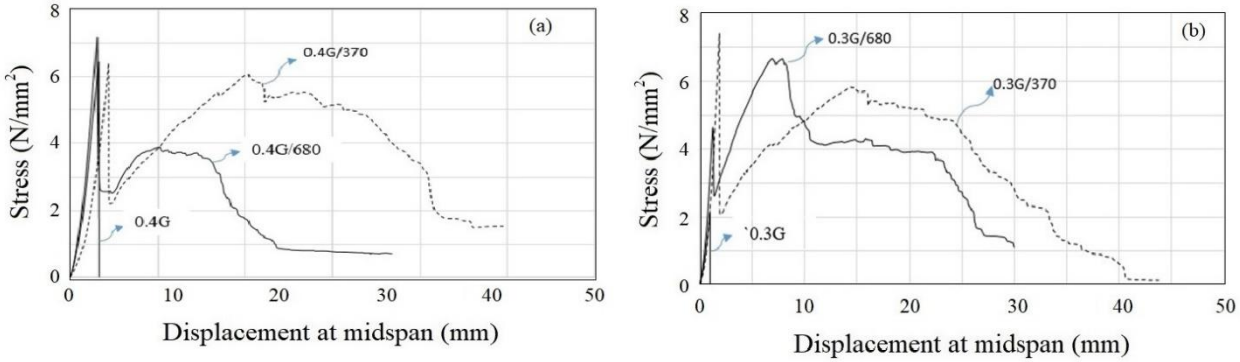

Fig. 7 Comparison of flexural strength test of pure matrix and composite for selected samples: (a) 0.4G and (b) 0.3G

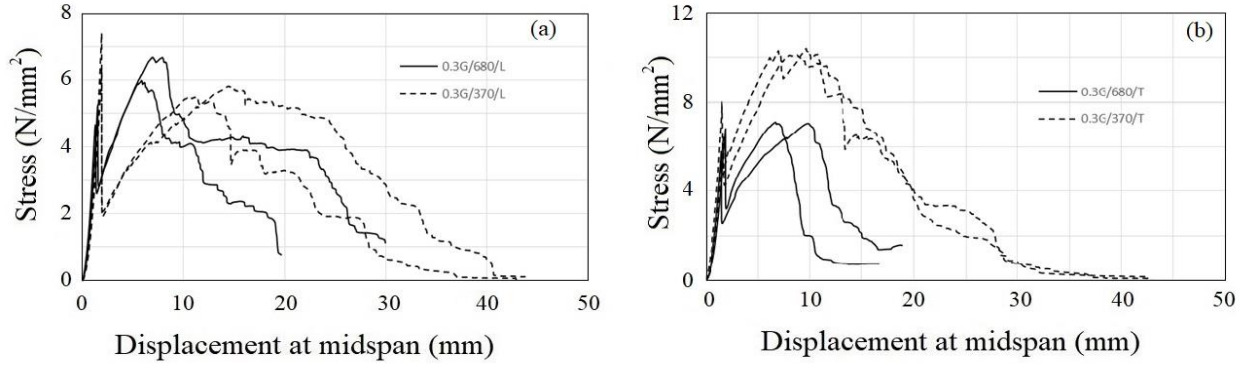

Fig. 8 Flexural strength test results of selected samples (a) 0.1G/250/T, (b) 0.4G/250/T, (c) 0.4G/250/T and (d) 0.4G/250/L

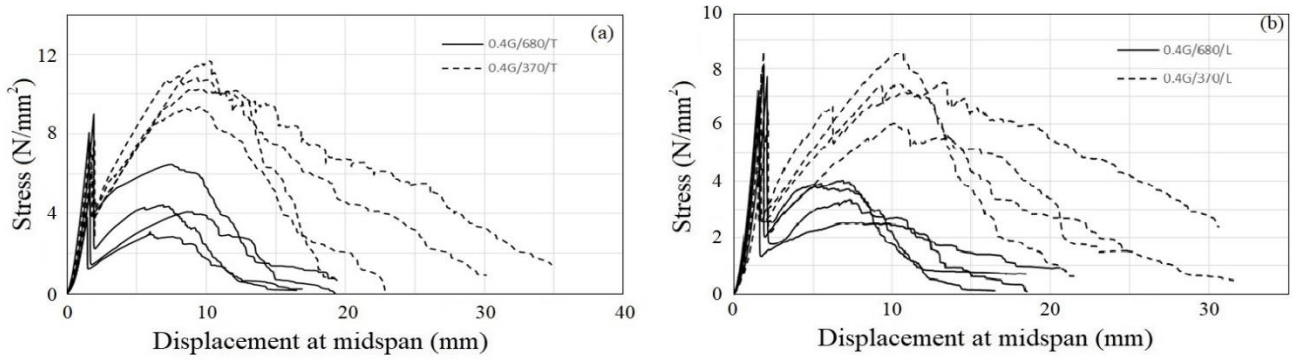

Fig. 9 Effect of textile type on behavior of composite for selected samples: (a) 0.4G and (b) 0.3G

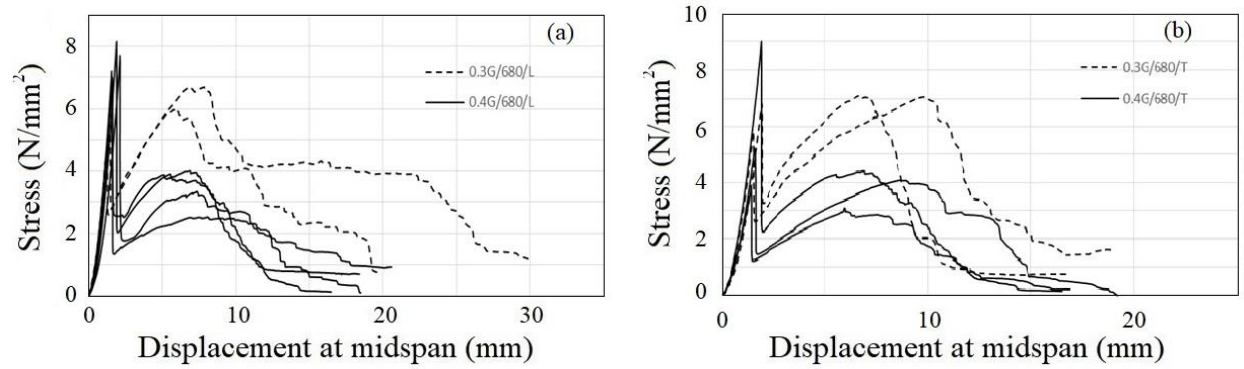

Fig. 10 Effect of matrix on behavior of composite for selected samples: (a) 0.4G and (b) 0.3G

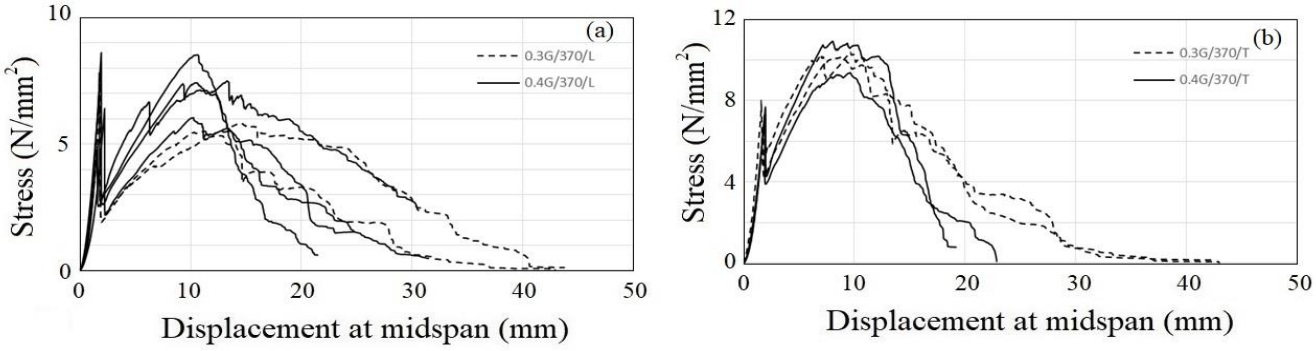

Fig. 11 Effect of matrix on behavior of composite for selected samples: (a) 0.4G and (b) 0.3G

Fig. 12 Microscopic textile damaged spots: (a) 0.3G/680/L and (b) 0.4G/680/L

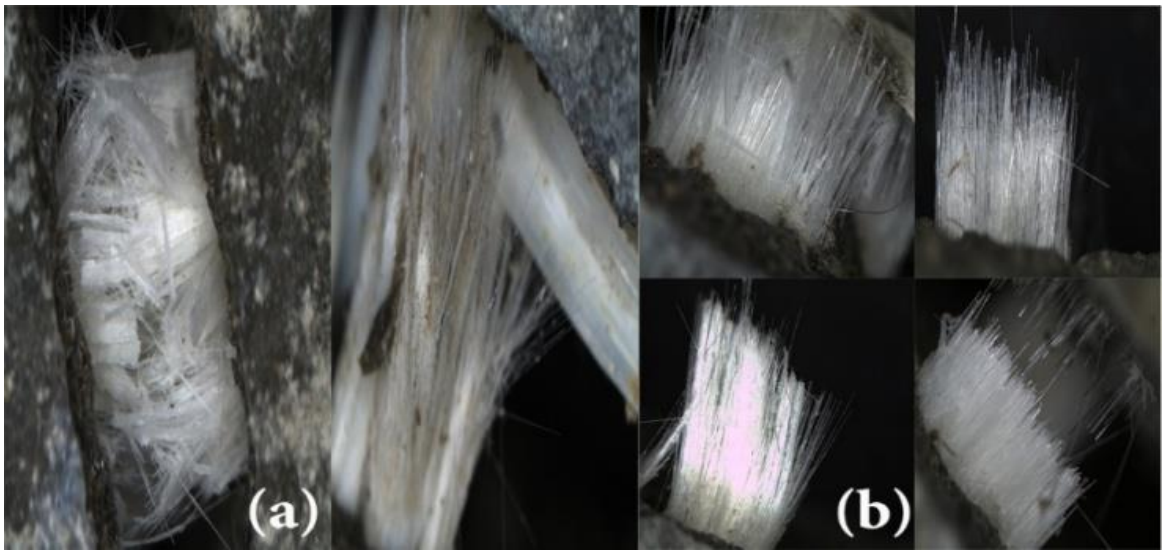

Fig. 13 Microscopic textile damaged spots: (a) 0.3G/680/T and (b) 0.4G/680/T

In Fig. 12, the presence of increased cementitious residue indicates strong bonding, enhancing the composite's ability to withstand higher loads during strain-hardening phases. Fig. 13(a) illustrates AR 680 glass textile showing mixed pullout and fracture behavior within the 0.3G matrix, enhancing its deformation capacity. This suggests a combined mechanism contributing to the composite's flexibility. Conversely, Fig. 13(b) shows AR 680 in the 0.4G matrix primarily experiencing fracture, reflecting robust bonding but limited deformation capacity before

Fig. 14 Microscopic textile damaged spots: (a) 0.3G/370/L and (b) 0.4G/370/L

Fig. 15 Microscopic textile damaged spots: (a) 0.3G/370/T and (b) 0.4G/370/T

failure. Fig. 14 demonstrates enhanced bonding and pullout performance with increased cementitious residue on the glass textile. However, Fig. 15 reveals fracture failure mode in the glass textile across different matrix proportions, indicating consistent behavior under varying conditions. These observations highlight the critical role of bonding quality and textile behavior in influencing composite deformation and failure modes.

The study extensively examined how different glass textile types (AR 370 and AR 680) interacted with varying matrix compositions (0.3G and 0.4G), influencing mechanical properties significantly. AR 370 demonstrated higher load-bearing capacity and deformability, particularly effective in weaker matrices, while AR 680 exhibited a nuanced behavior with both pullout and fracture mechanisms evident. These observations highlighted the intricate matrix-textile interaction and emphasized how textile variations impact the composite's mechanical behavior. An important finding was the presence of increased cementitious residue on glass textiles, indicating superior bonding and enhancing pullout performance. The fracture behavior observed across different matrix compositions served as a critical indicator of structural integrity, underscoring the role of bonding strength in determining load-bearing capacity and overall mechanical performance.

Ductility is a critical property in structural engineering, particularly in seismic and high-stress applications, where materials must absorb and redistribute energy to prevent catastrophic failure. High ductility allows materials to undergo plastic deformation, enabling them to resist cracking and provide early warning signs of structural failure, thereby improving overall safety. In the context of glass textile-reinforced cementitious composites, ductility measures the material's capacity to maintain structural integrity under bending or tensile loads. Glass textiles, known for their flexibility and strength, enhance the composite's ability to stretch and deform without fracturing. This characteristic makes such composites suitable for applications requiring resilience against dynamic loads, such as earthquakes or high wind conditions.

Energy dissipation capacity is a measure of a material's

ability to absorb and dissipate energy during deformation. It is particularly important in structures subjected to cyclic or dynamic loading, such as during seismic events. In the case of glass textile-reinforced composites, energy dissipation is achieved through mechanisms such as micro-cracking, matrix cracking, and textile elongation. These processes prevent the sudden release of energy, enabling the structure to absorb impacts and shocks gradually. Assessing this parameter provides insights into the composite's behavior under repetitive or extreme loading conditions, ensuring its reliability in high-stress environments.

From the three-point bending test, the ductility of the composite could be quantified using the ratio of deflection at failure to the elastic limit deflection. For instance, a ductility ratio of 8.5 could indicate exceptional capacity for deformation before failure. Such results highlight the composite's suitability for applications requiring significant energy absorption under bending forces.

- *Energy Dissipation Capacity*: Energy dissipation capacity could be accessed through cyclic loading tests. The composite dissipate 800J of energy per cycle before cracking, compared to 400J for traditional reinforced cementitious composites. This 50% improvement demonstrates the enhanced ability of glass textile reinforcement to absorb and redistribute energy, minimizing structural damage under dynamic loading.
- *Performance in UCS*: The UCS test reveal a slight trade-off with ductility. The composite achieve an average UCS of 6 to 8 MPa, marginally lower than conventional materials (12-15 MPa). However, this trade-off is offset by the superior ductility and energy dissipation properties, making the composite more adaptable to high-stress environments.

The above results suggest that while glass textile-reinforced composites may slightly lag in UCS compared to traditional materials, their significant improvements in ductility (e.g., 8.5 ratio) and energy dissipation capacity (e.g., 50% higher than conventional composites) make them a promising alternative for applications requiring resilience to dynamic forces.

5. Conclusions

The experimental analysis, particularly in bending tests, revealed distinct failure modes in the composites. Strong matrices led to textile rupture, resulting in lower energy absorption, while weaker matrices caused textile pullout. Key conclusions drawn from this study include:

- Impact of GGBFS: Incorporating GGBFS at 30% and 40% of total cement volume significantly enhanced concrete strength and improved bond strength between textiles and the matrix. GGBFS also acted as a mineral admixture, enhancing flowability beneficial for self-consolidating concrete.
- Relationship between Compressive and Flexural Strength: Matrices with higher compressive strength (e.g., 0.4G) exhibited superior performance in flexural testing, showing a direct correlation between compressive strength and flexural strength.
- Role of Textile Direction and Fiber Amount: Textile directionality significantly influenced load transfer, with both longitudinal and transverse tensile forces playing crucial roles. Higher fiber content in textiles was more impactful in stronger matrices, whereas in weaker matrices, fiber amount along the direction played a lesser role.
- Textile Quality and Matrix Influence: Stronger textiles with higher fiber content mitigated the influence of matrix quality, especially noticeable in weaker matrices where textile quality disparities were more pronounced.
- Role of Textile Density: Textile density emerged as a critical factor affecting composite behavior, influencing deflection-hardening and deflection-softening characteristics.

Acknowledgments

The authors declare that there are no conflicts of interest regarding the publication of this paper.

This work was supported by the Science and Technology projects of Education Government in Jiangxi province (Grant No. GJJ209406, GJJ218505, and GJJ218504), and the National Nature Sciences Foundation of China (Grant No. 42250410321).

References

Altun, F., Haktanir, T. and Ari, K. (2006), "Experimental investigation of steel fiber reinforced concrete box beams under bending", *Mater. Struct.*, **39**, 491-499. https://doi.org/10.1617/s11527-006-9095-y.

Amin, M., Zeyad, A.M., Tayeh, B.A. and Agwa, I.S. (2022), "Effect of ferrosilicon and silica fume on mechanical, durability, and microstructure characteristics of ultra high-performance concrete", *Constr. Build. Mater.*, **320**, 126233. https://doi.org/10.1016/j.conbuildmat.2021.126233.

Arunakanthi, E. and Kumar, J.C. (2016), "Experimental studies on fiber reinforced concrete (FRC)", *Int. J. Civil Eng. Technol.*, **7**(5), 329-336.

ASTM C39/C39M (2021), *Standard Test Method for Compressive Strength of Cylindrical Concrete Specimens*. ASTM International, West Con-shohocken, PA, USA.

ASTM C78 (2009), *Standard Test Method for Flexural Strength of Concrete (Using Simple Beam with Third-Point Loading)*. ASTM International, West Conshohocken, PA, USA.

Bencardino, F., Rizzuti, L., Spadea, G. and Swamy, R.N. (2010), "Experimental evaluation of fiber reinforced concrete fracture properties", *Compos. B: Eng.*, **41**(1), 17-24. https://doi.org/10.1016/j.compositesb.2009.09.002.

Benimam, S., Bentchikou, M., Debieb, F., Kenai, S. and Guendouz, M. (2021), "Physical and mechanical properties of cement mortar with LLDPE powder and PET fiber wastes", *Adv. Concrete Constr.*, **12**(6), 461-467. https://doi.org/10.12989/acc.2021.12.6.461.

Cemiloglu, A., Zhu, L., Arslan, S., Xu, J., Yuan, X., Azarafza, M.

and Derakhshani, R. (2023), "Support vector machine (SVM) application for uniaxial compression strength (UCS) prediction: A case study for Maragheh limestone", *Appl. Sci*., **13**(4), 2217. https://doi.org/10.3390/app13042217.

Doyon-Barbant, J. and Charron, J.P. (2018), "Impact of fibre orientation on tensile, bending and shear behaviors of a steel fibre reinforced concrete", *Mater. Struct*., **51**, 1-16. https://doi.org/10.1617/s11527-018-1282-0.

Gao, X., Li, D., Wu, W. and Chen, S. (2018), "Experimental investigation of the tensile and bending behavior of multi-axial warp-knitted fabric composites", *Textile Res. J*., **88**(3), 333-344. https://doi.org/10.1177/0040517516679915.

Guleria, A.N. and Salhotra, S. (2016), "Effects of silica fume (micro silica or nano silica) on mechanical properties of concrete: A review", *Int. J. Civ. Eng. Technol*., **7**(4), 345-357.

Hang, Z., Feng, C., Shen, L., Unluer, C. and Wang, S. (2024), "Experimental and theoretical analysis on the thermomechanical properties of functionally graded graphene nanoplatelet reinforced cement composites", *Cement. Concrete Compos*., **153**, 105740. https://doi.org/10.1016/j.cemconcomp.2024.105740.

Hassan, A.M.T., Jones, S.W. and Mahmud, G.H. (2012), "Experimental test methods to determine the uniaxial tensile and compressive behaviour of ultra high performance fibre reinforced concrete (UHPFRC)", *Constr. Build. Mater.*, **37**, 874-882. https://doi.org/10.1016/j.conbuildmat.2012.04.030.

Kansal, C.M. and Goyal, R. (2021), "Analysing mechanical properties of concrete with nano silica, silica fume and steel slag", *Mater. Today: Proceedings*, **45**, 4520-4525. https://doi.org/10.1016/j.matpr.2020.12.1032.

Khan, M., Anwar, W., Rasheed, M., Najeh, T., Gamil, Y. and Farooq, F. (2024), "Forecasting the strength of graphene nanoparticles-reinforced cementitious composites using ensemble learning algorithms", *Results Eng*., **21**, 101837. https://doi.org/10.1016/j.rineng.2024.101837.

Khanzadi, M. and Behnood, A. (2009), "Mechanical properties of high-strength concrete incorporating copper slag as coarse aggregate", *Constr. Build. Mater.*, **23**(6), 2183-2188. https://doi.org/10.1016/j.conbuildmat.2008.12.005.

Kontoni, D.P.N., Jahangiri, B., Dalvand, A. and Shokri-Rad, M. (2023), "Effect of length and content of steel fibers on the flexural and impact performance of self-compacting cementitious composite panels", *Adv. Concrete Constr.*, **15**(1), 23-39. https://doi.org/10.12989/acc.2023.15.1.023.

Lho, B.C., Joo, M.K., Choi, K.H. and Choi, J.Y. (2012), "Effects of polymer-binder ratio and slag content on strength properties of autoclaved polymer-modified concrete", *KSCE J. Civil Eng*., **16**, 803-808. https://doi.org/10.1007/s12205-012-1373-3.

Liao, Q., Guo, Z.W., Duan, X.Z., Yu, J.T., Liu, K.K. and Dong, F. Y. (2021), "Mechanical behavior and chloride resistance of cementitious composites with PE and steel fiber", *Adv. Concrete Constr*., **12**(6), 451-459. https://doi.org/10.12989/acc.2021.12.6.451.

Liu, S., Cao, S., Hao, Y., Chen, P. and Ma, G. (2024), "Prediction models of compressive mechanical properties of steel fiber-reinforced cementitious composites (SFRCC)", *J. Build. Eng*., **84**, 108629. https://doi.org/10.1016/j.jobe.2024.108629.

Liu, Y., Shi, C., Zhang, Z., Li, N. and Shi, D. (2020), "Mechanical and fracture properties of ultra-high performance geopolymer concrete: Effects of steel fiber and silica fume", *Cement Concrete Compos.*, **112**, 103665. https://doi.org/10.1016/j.cemconcomp.2020.103665.

Luo, X., Si, Y. and Gu, W. (2019), "Effect of silica fume on mechanical properties of concrete incorporating steel slag powder", *Wuhan Uni. J. Nat. Sci*., **24**, 86-92. https://doi.org/10.1007/s11859-019-1372-z.

Marthong, C. (2019), "Effect of waste cement bag fibers on the mechanical strength of concrete", *Adv. Mater. Res*., **8**(2), 103-115. https://doi.org/10.12989/amr.2019.8.2.103.

Mindess, S. and Bentur, A. (1990), *Fibre Reinforced Cementitious Composites*. Modern Concrete Technology Series press.

Mobasher, B. (2011), *Mechanics of Fiber and Textile Reinforced Cement Composite*. CRC Press.

Mudadu, A., Tiberti, G., Plizzari, G.A. and Morbi, A. (2019), "Post-cracking behavior of polypropylene fiber reinforced concrete under bending and uniaxial tensile tests", *Struct. Concrete*, **20**(4), 1411-1424. https://doi.org/10.1002/suco.201800224.

Nanehkaran, Y.A., Azarafza, M., Pusatli, T., Bonab, M.H., Irani, A. E., Kouhdarag, M. and Derakhshani, R. (2023), "Deep learning method for compressive strength prediction for lightweight concrete", *Comput. Concrete*, **32**(3), 327. https://doi.org/10.12989/cac.2023.32.3.327.

Noghabai, K. (2000). Beams of fibrous concrete in shear and bending: Experiment and model. *J. Struct. Eng*., **126**(2), 243-251. https://doi.org/10.1061/(ASCE)0733-9445(2000)126:2(243).

Noshiravani, T. and Brühwiler, E. (2013), "Experimental investigation on reinforced ultra-high-performance fiber-reinforced concrete composite beams subjected to combined bending and shear", *ACI Struct. J*., **110**, 251-261.

Olivito, R.S. and Zuccarello, F.A. (2010), "An experimental study on the tensile strength of steel fiber reinforced concrete", *Compos. Part B: Eng*., **41**(3), 246-255. https://doi.org/10.1016/j.compositesb.2009.12.003.

Pan, J., Ping, P., Ding, B., Zhu, B., Lin, Y., Ukrainczyk, N. and Cai, J. (2024), "Impact behaviour of 3D printed fiber reinforced cementitious composite beams", *Compos. A: Appl. Sci. Manufact*., **182**, 108175. https://doi.org/10.1016/j.compositesa.2024.108175.

Richardson, D.N. (2006), *Strength and durability characteristics of a 70% ground granulated blast furnace slag (GGBFS) concrete mix*. Missouri Department of Transportation Organizational Results Final Report, **12**(2), 85-98.

Tailhan, J.L., Rossi, P. and Boulay, C. (2012), "Tensile and bending behaviour of a strain hardening cement-based composite: experimental and numerical analysis", *Cement Concrete Compos*., **34**(2), 166-171. https://doi.org/10.1016/j.cemconcomp.2011.10.005.

Travush, V.I., Karpenko, N.I., Kolchunov, V.I., Kaprielov, S.S., Demyanov, A.I., Bulkin, S.A. and Moskovtseva, V.S. (2020), "Results of experimental studies of high-strength fiber reinforced concrete beams with round cross-sections under combined bending and torsion", *Struct. Mech. Eng. Constr. Build*., **16**(4), 290-297. https://doi.org/10.22363/1815-5235-2020-16-4-290-297.

Türkmen, İ.I.M., Gül, R., Çel, C. and Demrboğa, R. (2003), "Determination by the Taguchi method of optimum conditions for mechanical properties of high strength concrete with admixtures of silica fume and blast furnace slag", *Civil Eng. Environ. Syst*., **20**(2), 105-118. https://doi.org/10.1080/1028660031000081527.

Wang, Y., Zhang, S., Niu, D., Su, L. and Luo, D. (2019), "Effects of silica fume and blast furnace slag on the mechanical properties and chloride ion distribution of coral aggregate concrete", *Constr. Build. Mater.*, **214**, 648-658. https://doi.org/10.1016/j.conbuildmat.2019.04.149.

Wu, L. S., Yu, Z.H., Zhang, C. and Bangi, T. (2022), "Mechanical properties and assessment of a hybrid ultra-high-performance engineered cementitious composite using calcium carbonate whiskers and polyethylene fibers", *Comput. Concrete*, **30**(5), 339-355. https://doi.org/10.12989/cac.2022.30.5.339.

Wu, X., Cai, Z., Xie, Q., Chai, X., Yu, K. and Chen, W. (2024), "Tensile behavior of high-performance hybrid steel-basalt fibers

reinforced cementitious composites after high-temperature exposure", *Constr. Build. Mater.*, **426**, 136059. https://doi.org/10.1016/j.conbuildmat.2024.136059.

Xu, H., Shao, Z., Wang, Z., Cai, L., Li, Z., Jin, H. and Chen, T. (2020), "Experimental study on mechanical properties of fiber reinforced concrete: Effect of cellulose fiber, polyvinyl alcohol fiber and polyolefin fiber", *Constr. Build. Mater.*, **261**, 20610. https://doi.org/10.1016/j.conbuildmat.2020.120610.

Yoo, D.Y., Kim, S., Kim, J.J. and Chun, B. (2019), "An experimental study on pullout and tensile behavior of ultra-high-performance concrete reinforced with various steel fibers", *Constr.. Build. Mater.*, **206**, 46-61. https://doi.org/10.1016/j.conbuildmat.2019.02.058.